Review of Contemporary Philosophy ISSN: 1841-5261, e-ISSN: 2471-089X

Vol 22 (1), 2023 Pp 1315 - 1330



Emerging Applications of Dual-Energy CT in Diagnostic Radiology-An Updated Review of Urological Assessment.

¹-Ahmed Haidar Badidi, ²-Tahani Mohammed Hakami, ³- Hamdan Ali Hamdan Alghamdi, ⁴- Nawaf Jaber Aljohani, ⁵- Mohammad Johar Alanbar, ⁶- Abdulmajed Nawaf N Alotabi, ⁻-Abeer Abdullah Aljamaan, ³- Suleman Abdu Alhunishi, ॰-Yousef Damigh Aldamigh, ¹¹ - Mohammad Abdulaziz Alhelyel, ¹¹ Abdullah Mansour Ali Akkam, ¹²-Mohammed Hassan Alshehri, ¹³-Ammar Ali Hakami, ¹⁴-Nadha Fahad Alhumaydani, ¹⁵-Gawaher Saadallah Almotiri,

- 1. Ksa, Ministry of Health, Abu Arish general hosbital
- ^{2.} Ksa, Ministry of Health, King Salman bin Abdulaziz in Riyadh Hospital
 - 3. Ksa, Ministry of Health, Aqiq General Hospital
 - 4. Ksa, Ministry of Health, The first health cluster in Riyadh
 - 5. Ksa, Ministry of Health, Aloun general hospital
 - ^{6.} Ksa, Ministry of Health, Forensics Medical Services Center, Riyadh
 - 7. Ksa, Ministry of Health, King salman Hospital
 - 8. Ksa, Ministry of Health, Muhayl General Hospital
 - 9. Ksa, Ministry of Health, The second health cluster
 - ^{10.} Ksa, Ministry of Health, Hawtat sudayr hospital
 - ^{11.} Ksa, Ministry of Health, King Salman bin Abdul Aziz.
 - ^{12.} Ksa, Ministry of Health, Thurayban General Hospital
 - 13. Ksa, Ministry of Health, Jazan Health Complex
- 14. Ksa, Ministry of Health, King Salman bin Abdulaziz in Riyadh Hospital
- ^{15.} Ksa, Ministry of Health, King Salman bin Abdulaziz in Riyadh Hospital

Background: Dual-energy computed tomography (DECT) has emerged as an advanced imaging technology in diagnostic radiology, particularly in urological assessment. It overcomes several limitations inherent in traditional CT scans by utilizing two different energy levels, providing enhanced tissue characterization and improved contrast resolution. DECT has shown great promise in evaluating urinary tract diseases, offering precise data on morphology, function, and content, thus enhancing clinical decision-making.

Aim: This review aims to explore the principles, benefits, and clinical applications of DECT in the evaluation of urological disorders, focusing particularly on urinary stone characterization.

Methods: The review synthesizes data from various studies investigating the use of DECT in urological imaging, with a particular emphasis on urinary stone analysis. Various DECT technologies, such as dual-source CT and spectral imaging, are discussed, highlighting their ability to differentiate between stone compositions and their clinical relevance.

Results: DECT offers multiple advantages in urological assessment, such as virtual monochromatic images (VMIs), virtual non-contrast enhanced images, iodine maps, and spectral Hounsfield unit (HU) curves. These capabilities enhance the detection and characterization of urinary stones, including distinguishing uric acid stones from non-uric acid stones with high sensitivity and specificity. Studies have demonstrated that DECT provides improved diagnostic accuracy compared to traditional CT, particularly in identifying stone composition, and reducing radiation exposure.

Conclusion: DECT represents a significant advancement in urological diagnostic imaging, improving the accuracy of urinary stone characterization, reducing radiation exposure, and offering comprehensive tissue

analysis. It enhances clinical management by enabling precise differentiation between stone types and optimizing treatment strategies.

Keywords: Dual-energy CT, urology, urinary stones, diagnostic radiology, virtual monochromatic images, iodine maps, radiation reduction, tissue characterization, nephrolithiasis.

Received: 07 october 2023 Revised: 22 November 2023 Accepted: 06 December 2023

Introduction:

Computed tomography (CT) is a non-invasive imaging modality that use X-rays to get detailed images of inside anatomical structures. CT scans facilitate doctors in identifying and describing a wide range of genitourinary disorders, such as renal stones, abnormal renal parenchyma, and renal lesions, hence aiding in the selection of the most suitable treatment [1]. Nonetheless, conventional CT imaging possesses certain limitations in the evaluation of urological diseases [2]. Dual-energy CT (DECT) is a sophisticated technology that improves the visibility and characterisation of tissues through the use of two different energy levels of X-rays. This technology has emerged as a valuable instrument for assessing urinary tract illnesses, providing accurate data on the morphology, function, and content of the urinary system, while mitigating certain limitations associated with traditional CT scans [4]. This paper analyzes the concepts, benefits, and prospective clinical applications of DECT in the investigation of urinary tract problems.

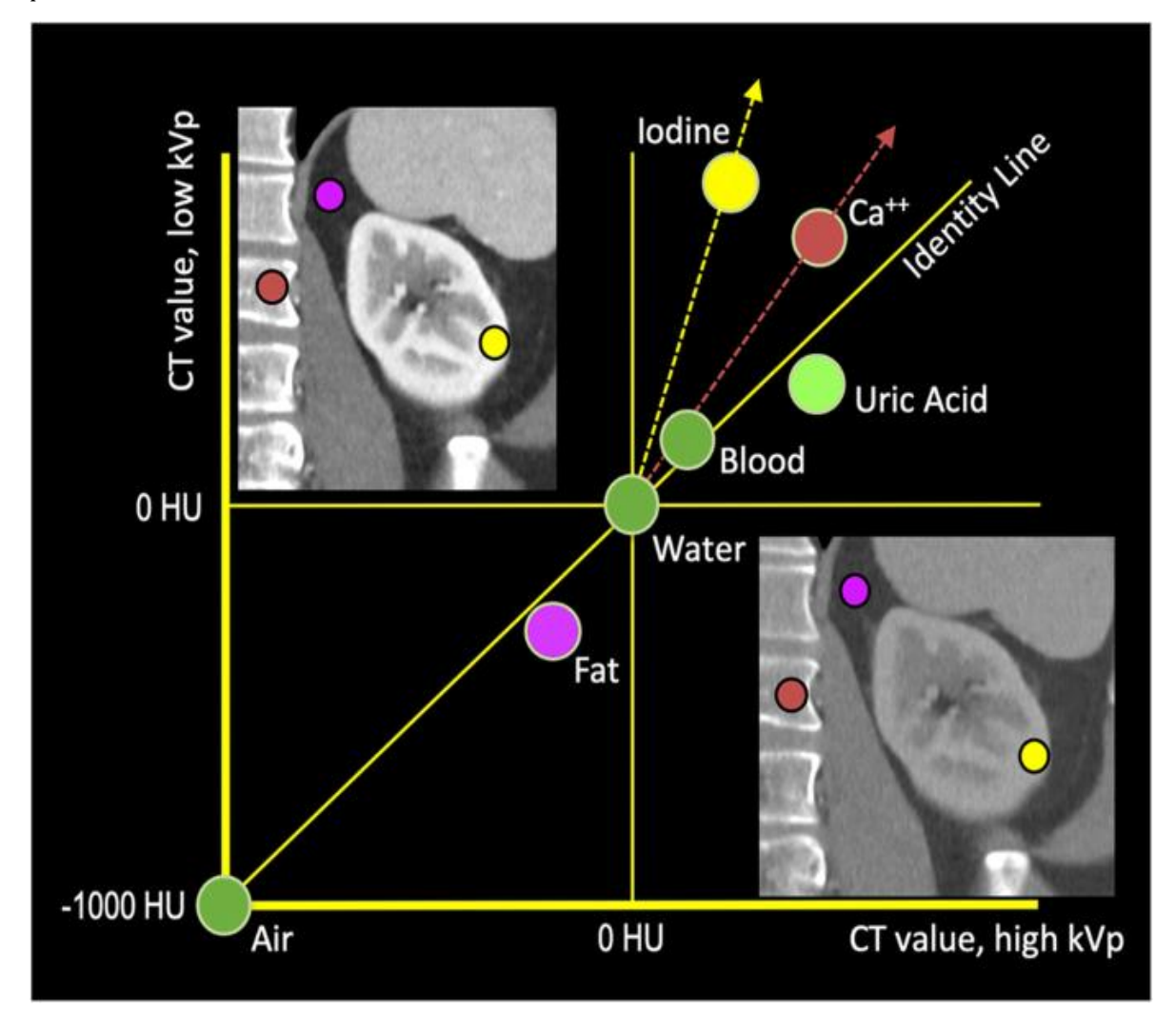


Figure 1: Dual-Energy Protocol for Routine Scan.

Principles of DECT:

CT scanners produce X-rays by directing an electron beam from the cathode onto a concentrated focal point of the tungsten target anode. This process produces X-rays that encompass a wide variety of energy, referred to as "polychromatic X-rays," constituting the X-ray spectrum. The peak photon energy in this spectrum is equivalent to the kilovoltage of the X-ray tube; for example, a 120 kV tube has a maximum energy of 120 keV. The X-ray spectrum is contingent upon tube voltage, with the effective X-ray energy acting as a typical metric for a polychromatic X-ray spectrum [5]. The effective energy refers to a monochromatic X-ray energy that generates analogous interactions, which can be quantified using an absorber like aluminum or copper [6].

In DECT, virtual monochrome images (VMIs) acquired at 65–70 keV exhibit identical CT attenuation values (Hounsfield units, HU) to those of single-energy CT images captured at 120 kVp [7]. These VMIs offer information approximately equivalent to single-energy CT pictures at 120 kVp. The fundamental idea of DECT is its capacity to attain improved contrast resolution among various materials by utilizing their distinct spectrum characteristics, including the differential attenuation of X-rays at differing photon energies. The CT number (HU) of a material varies with different energy levels, influenced by its component composition. CT numbers correlate with a material's linear attenuation coefficient and are not universally distinctive for each substance, as other materials may display analogous CT numbers. The overlap in CT densities complicates the differentiation of materials in single-energy CT scans, providing limited information regarding tissue composition [8]. Conversely, DECT pictures facilitate the distinction and quantification of materials with diverse elemental compositions by analyzing their CT numbers at two separate energy levels, rendering DECT a potent instrument for evaluating tissue samples.

A variety of dual-energy technologies exist. Dual-energy CT often utilizes two separate X-ray energy levels, specifically between the 70–100 kVp and 135–150 kVp ranges. Certain systems employ independent X-ray sources using rapid tube-voltage modulation, sequential scanning, or dual-source CT configurations [9]. Alternative systems employ a singular X-ray source, dividing the beam into low- and high-energy bands either at the detector stage (dual-layer system) [10] or at the tube output (split filter system).

DECT data analysis can be categorized into image-based and raw data-based methodologies. Image-based analysis entails the post-processing of dual-energy scans before to or subsequent to the reconstruction of high- and low-energy pictures to provide diverse DECT applications [11]. This approach prioritizes the spatial alignment of reconstructed images over precise X-ray path matching for both high and low tube voltages. Post-reconstruction dual-energy data are processed to create blended images, which are weighted averages of images obtained from different tube voltages. Applications like iodine map images and virtual non-contrast images are generated by removing iodine map images from composite images. Conversely, raw data-based analysis necessitates exact alignment of X-ray trajectories for both high and low tube voltages. The unprocessed data, including iodine and water or bone and water, undergoes direct material degradation, then followed by picture reconstruction. This method presupposes that the body comprises a blend of substances, including iodine and water, and determines the makeup of each from the initial raw data. Analysis based on raw data enables a wider array of DECT applications compared to analysis based on images. Methods such as VMI, electron density, and effective atomic-number analyses depend on the examination of raw data. The selection between raw data analysis and image-based analysis is contingent upon the DECT hardware; raw data analysis is generally utilized in systems including rapid tube-voltage switching, sequential scanning, and dual-layer detector systems, whilst image-based analysis is applied in dual-source CTscanners.

Advantages of DECT

Dual-energy CT provides numerous benefits applicable in clinical practice.

Virtual Monochromatic Imagery:

Virtual monochrome images (VMIs) replicate images produced by monochromatic X-rays at any specified energy level. VMIs at around 65-70 keV are frequently chosen as standard pictures due to their

CT attenuation values resembling those obtained from single-energy CT scans at 120 kVp [12]. VMIs at this energy levels typically demonstrate reduced picture noise [13]. Analogous to single-energy CT scans conducted at reduced tube voltages, VMIs obtained at diminished energy levels (e.g., below 60 keV) augment iodine contrast, hence improving the discernibility of contrast-enhanced lesions. This attribute decreases the necessary contrast medium dosage by 40–60% when employing VMIs at 40–50 keV, especially advantageous for individuals with renal failure [14]. Moreover, reduced energy levels enhance X-ray absorption by iodine, especially near its k-edge (33.2 keV), hence facilitating the identification of hypervascular lesions, including primary renal-cell carcinomas and their metastatic sites [4,15,16,17].

Virtual Non-Contrast Enhanced Images

Attenuation measurements obtained at the second energy level enable the decomposition of a mixture of materials into its constituent elements, which is fundamental in generating virtual non-contrast enhanced (VNC) and iodine images. VNC images are produced by subtracting iodine from contrast-enhanced DECT images via three-material decomposition [18]. These images facilitate the distinction of calcifications or high-attenuation materials from iodine-enhanced tissues. The generation of VNC images, as opposed to acquiring actual unenhanced images, allows for a reduction in radiation exposure when unenhanced CT scans are necessary [19].

Iodine Maps

Iodine is a crucial contrast agent in CT scans, improving the visibility of blood vessels, cancers, and other diseases. The iodine map provides comprehensive information regarding the distribution and concentration of iodine in tissues [20]. This map is essential for analyzing iodine absorption, defining lesions, assessing tumor vascularity, and monitoring therapeutic response. Iodine maps, usually presented in color, emphasize places with elevated iodine concentrations through richer hues, hence enabling straightforward identification of iodine-rich areas. Furthermore, iodine maps improve the identification of extraluminal iodine elements, hence facilitating the detection of urine leakage, whether resulting from trauma [21] or iatrogenic injury [22].

Spectral HU Curves

VMIs can be utilized to produce spectral Hounsfield unit (HU) curves by defining a region of interest (ROI) within a tissue and recording the average CT number at each monochromatic energy level of the VMI, generally ranging from 40 to 140 keV. Spectral HU curves offer critical insights into the attenuation characteristics of tissues inside the ROI, aiding in tissue characterisation and enhancing differential diagnoses. At diminished energy levels, soft tissues and high atomic number substances, like iodine and bone, demonstrate heightened attenuation, whereas fat displays decreased attenuation. This attenuation pattern facilitates the diagnosis of fat-containing pathologies, such as lipid-rich plaques, adrenal adenomas, and angiomyolipomas (AML) [4].

DECT Clinical Applications

This section presents an overview of DECT's potential clinical applications, particularly in the context of urological disorders.

Characterization of Urinary Stones

CT imaging is the definitive standard for identifying nephrolithiasis, with non-enhanced scans demonstrating sensitivities and specificities of 95% [23,24]. CT is increasingly employed for the urgent assessment of urinary calculi, as it can help identify other conditions that contribute to acute abdominal pain. Uric acid stones, consisting of elements with lower atomic numbers such as carbon, hydrogen, nitrogen, and oxygen, contrast with non-uric acid stones, which are comprised of elements with higher atomic numbers like calcium, sulfur, and phosphorus [25]. Conventional CT can elucidate stone composition using HU attenuation measurements; however, the considerable overlap in HU values among various stone kinds restricts its diagnostic efficacy. Uric acid stones generally have HU values ranging from 200 to 400, whereas calcium oxalate stones fall between 600 and 1200 [26,27]. This overlap can impede precise

diagnosis and treatment choices, as the detection of uric acid stones frequently leads to medicinal dissolving therapy instead of surgical surgery [28].

DECT improves stone composition analysis by distinguishing stone kinds according to their attenuation ratios at varying energy levels. The attenuation ratio at 80 kVp to 140 kVp is computed using dual-source DECT and compared to established stone composition profiles. The three-material decomposition approach, which posits that each voxel comprises constituents like water, calcium, or uric acid, aids in the classification of stone forms. The software rapidly analyzes this data, designating uric acid stones in red and non-uric acid stones in blue [29]. Rapid kilovoltage switching apparatus facilitates enhanced distinction by graphing effective atomic numbers versus attenuation patterns to differentiate among uric acid, calcium oxalate, cystine, or struvite calculi [30]. The distinct attenuation variations between high- and low-energy spectra facilitate the separation of materials possessing analogous electron concentrations yet differing photon absorption properties. Post-processing techniques, such as material decomposition algorithms, facilitate the examination of stones with mixed compositions, enabling the detection of trace amounts of certain components inside the stone [31]. A standard DECT protocol for nephrolithiasis entails an initial low-dose conventional CT scan to detect possible urinary stones, succeeded by a DECT scan concentrating on the stone's location. The obtained images undergo processing via a threematerial decomposition method, which allocates color codes according to stone composition, hence enabling precise identification and characterisation of the stones [32].

Employing the previously indicated acquisition methodology, Thomas et al. established an effective radiation dosage between 3.4 and 5.3 mSv [33]. Jepperson et al. conducted a comparative study examining the radiation exposure linked to DECT protocols in relation to low-dose and conventional CT scans. No significant change in radiation exposure was seen when comparing DECT to low-dose CT alone. DECT procedures at 80/140 kVp and 100/140 kVp achieved a 40% and 31% reduction in radiation exposure, respectively, in comparison to standard CT scans [34].

Numerous studies have assessed the precision of DECT in the characterisation of urinary calculi. Spek et al. examined 213 stones from 64 patients and discovered that uric acid (UA)-containing stones displayed a markedly distinct dual-energy index (p = 0.001) when compared to pure calcium (0.073) and mixed calcium stones (0.077), attaining a sensitivity of 98.4% and a specificity of 98.1% in distinguishing uric acid stones from non-uric acid stones [35]. Lombardo et al. assessed DECT images from 33 patients with 62 stones, whether spontaneously passed or treated, achieving 100% sensitivity and specificity in identifying both UA stones and non-UA stones [36]. Bonatti et al. evaluated nephrolithiasis patients who received a low-dose CT scan followed by a DECT scan, revealing that conventional CT accurately identified stone composition in 52% (26/50) of instances, whereas DECT identified 90% (45/50) of stones. Moreover, DECT accurately distinguished uric-acid stones from non-uric-acid stones in 96% (48/50) of instances, in contrast to 80% (40/50) with conventional CT [37].

Nestler et al. conducted a prospective investigation with 84 patients, revealing that DECT results exhibited 98.6% concordance with infrared spectrometry, alongside a sensitivity of 84.6%, specificity of 100%, positive predictive value of 100%, and negative predictive value of 98.5%. They additionally noted that the integration of urine pH with DECT improved diagnostic precision, attaining an area under the curve of 0.97, as contrast to 0.92 for DECT alone [38]. Euler et al. retrospectively analyzed 227 stones from 203 patients who received low-dose unenhanced dual-energy computed tomography for the identification and monitoring of urolithiasis. Employing X-ray diffraction as the reference standard, they accurately categorized 225 out of 227 stones, achieving pooled sensitivity, specificity, and accuracy of 1.0 (95% CI: 0.97, 1.00), 0.93 (95% CI: 0.68, 1.00), and 0.99 (95% CI: 0.97, 1.00), respectively. Moreover, 82 out of 84 stones with a diameter of ≤ 3 mm were precisely categorized [39].

Although DECT is highly effective, its accuracy may be somewhat reduced in patients with significant body habitus or when stones are smaller than 3 mm [40,41]. Nonetheless, this is generally not a clinically relevant issue, as stones smaller than 3 mm often do not necessitate intervention and are likely to pass spontaneously. The detection rate of stones is markedly affected by the content of iodine in the urine.

In a phantom study, more than 95% of 2–4 mm calculi in a diluted iodinated contrast medium solution were detectable on VNC pictures. The detection rate significantly decreased when stones were immersed in a highly concentrated iodine solution. Excessively iodinated urine may impede iodine subtraction in VNC, resulting in diminished sensitivity for stone detection when the iodine solution's attenuation value attains its maximum CT value in low-kV pictures [42].

In a comparison of VNC images produced during nephrographic and pyelographic phases, the sensitivity for stone detection was 77.5% in the nephrographic phase and 73.8% in the urographic phase (59/80). Elevated iodine levels in the excretory system may result in inadequate iodine subtraction on VNC images, leading to a bright rim along the collecting system that could obscure or misidentify stones [42]. The sensitivity of VNC in stone detection relies on the dimensions of the stones and the iodine concentration within the excretory system [4]. Incorporating both nephrographic and pyelographic phases in the acquisition technique allows for the generation of VNC from the nephrographic phase, which can alleviate complications associated with iodine density in the collecting system [43]. When employing a single pyelographic phase with a split-bolus technique, the protocol must be modified to achieve a reduced iodine concentration in the excretory system while ensuring adequate distension, either by administering a smaller volume of contrast material or by utilizing diuretics or patient hydration [44]. A further disadvantage of VNC images is that stones frequently appear diminished in size relative to authentic unenhanced photos [42,43]. Yeo et al. proposed enhancing the split-bolus technique by delivering 500 mL of water 30 minutes prior to DECT acquisition, followed by 50 mL and an additional 100 mL of contrast material after 540 seconds at a rate of 2 mL/s, along with a saline bolus of 40 mL. This method, utilized for patients with suspected urinary calculi, attained a sensitivity of 95.1% and a diagnostic accuracy of 92.9% for stone identification [45]. Ureteral stents and percutaneous nephrostomy tubes may sometimes obscure results. A research assessing 36 stents from seven manufacturers revealed that polyurethane stents exhibited a blue hue, but silicon stents displayed a red hue [46]. This information can aid urologists in choosing stents with an inverse color sequence when addressing particular stone types. When a stone is next to a stent, post-processing software may erroneously incorporate stent material into the stone composition analysis, resulting in mischaracterization, with a reported misdiagnosis rate of 4% to 8% [47].

Study of Renal Lesions

Numerous renal lesions discovered incidentally may be insufficiently detected using conventional CT imaging, presenting difficulties for both radiologists and referring physicians. Dual-energy computed tomography (DECT) provides substantial benefits in the characterization of renal lesions, improving diagnostic confidence and minimizing the necessity for supplementary imaging relative to traditional single-energy dual-phase CT, while preserving diagnostic efficacy comparable to magnetic resonance imaging (MRI) [54]. DECT may function as an alternate diagnostic modality for identifying enhanced renal lesions, especially in patients who struggle with breath-holding or cannot endure extended MRI examination durations, potentially resulting in unsatisfactory precontrast and postcontrast acquisitions. DECT is appropriate for patients with pacemakers or other contraindications to MRI [55,56]. In standard contrast-enhanced CT, renal lesions with attenuation levels akin to water are often classified as simple cysts. A dual-phase method, comprising one phase prior to and one phase subsequent to the administration of intravenous contrast, is necessary to distinguish whether a lesion with attenuation above that of water is a non-enhancing hyperdense cyst or an enhancing solid mass [57]. The disparity in attenuation among these stages dictates the enhancement of a lesion: many radiologists define enhancement as a rise of 10 Hounsfield units (HU), whilst others regard a 20 HU increase as definitive enhancement [57].

Virtual non-contrast (VNC) pictures produced from improved dual-energy computed tomography (DECT) scans exhibit a robust association with authentic unenhanced images, with attenuation measures on VNC images closely resembling those of unenhanced scans [58]. Iodine maps, derived from material decomposition techniques in contrast-enhanced dual-energy computed tomography (DECT), serve as a dependable method for detecting enhancing lesions [59]. The maps illustrate iodine contrast within the examined voxels by color-coded overlays, enabling the distinction between non-enhancing renal cysts, which do not contain iodine, and enhancing solid renal tumors, which absorb the iodine contrast medium

[8,9,19]. Color-coded iodine overlays facilitate rapid visual differentiation between enhancing and non-enhancing renal lesions, proving especially beneficial in scenarios with multiple renal lesions, such as polycystic kidney disease, where enhancing lesions can be readily distinguished from cysts and hemorrhagic cysts [60]. Iodine maps have been effective in defining hyperdense renal masses discovered accidentally during single-phase enhanced DECT, especially for lesions of ≥1.5 cm [61]. DECT improves lesion characterisation by quantifying the iodine concentration in each picture pixel. DECT records also include spectral attenuation curves [62]. By delineating a region of interest (ROI) within a lesion, the lesion's attenuation characteristic across the multi-energy spectrum can be evaluated. Iodine-containing lesions demonstrate an increase in attenuation at lower energies ("upward-curve-type"), while cysts maintain a uniform attenuation level throughout the monochromatic multi-energy spectrum ("flat-curve-type") [9].

Moleesaide et al. conducted a study analyzing 78 renal incidental lesions (24 enhancing and 54 nonenhancing), measuring between 1 to 4 cm, employing rapid kilovoltage-switching dual-energy computed tomography (DECT), with results compared to histological analysis. The analysis of monochromatic images and iodine curves significantly differentiated between enhancing and nonenhancing lesions (p < 0.001) [63]. The precise preoperative pathological classification of renal cell carcinoma (RCC) is crucial for evaluating tumor malignancy and selecting the appropriate surgical approach. DECT aids in assessing the vascular supply of tumors, as the characteristics of tumor blood supply correlate with pathological grade. For instance, well-differentiated clear-cell renal-cell carcinoma (ccRCC) typically exhibits mature arteries and heightened vascular permeability, whereas poorly differentiated ccRCC reveals hemodynamic anomalies and arteriovenous shunts [64]. Differentiating between papillary renal cell carcinoma (pRCC) and clear cell renal cell carcinoma (ccRCC) poses challenges with imaging modalities [65]. A recent study by Marcon et al. demonstrated that ccRCC exhibited much higher iodine levels than pRCC. A positive correlation is observed between iodine concentration and microvascular density on DECT. The study determined a threshold iodine concentration of ≤3.1 mg/mL, enabling the accurate identification of pRCC with an accuracy rate of 86.8% [56].

DECT is crucial for the characterization of angiomyolipoma (AML), typically identified by its macroscopic fat content. This can be corroborated through visual assessment and attenuation measurements of <-10 to -15 Hounsfield units (HU) on computed tomography (CT). However, misinterpretation may occur in cases of fat-poor acute myeloid leukemia (AML) or when imaging is limited to contrast-enhanced computed tomography (CT), due to elevated attenuation values. This may occur with small AMLs due to volume averaging with adjacent renal parenchyma or pseudo-enhancement, together with the presence of internal enhancing veins. As a result, around one-third of AMLs may remain indeterminate with HU measurements on contrast-enhanced CT, necessitating further imaging, such as specialized thin-section unenhanced CT or MRI, for confirmation. The implementation of DECT has led to the development of several analytical techniques, such as iodine maps, virtual monochrome imaging (VMI) with spectral curves, atomic-number maps, and fat maps, enhancing the sensitivity of CT in identifying intralesional adipose tissue. Material-specific fat images acquired from DECT have shown remarkable precision in detecting areas of macroscopic fat. Assessments of fat concentration provide a reliable means to confirm the presence of macroscopic fat in renal masses and to identify renal AML, even without noncontrast-enhanced CT. When DECT is utilized, the nodule can be definitively recognized as containing macroscopic fat without the need for further imaging [66]. In a prospective study involving 95 patients with renal tumors, researchers evaluated the absolute enhancement, enhancement ratio, and iodine concentration of each lesion in nephrographic phase imaging. They successfully distinguished fat-poor acute myeloid leukemias from renal neoplasms [67].

Study of the Bladder and Ureters

Urothelial tumors (UC) are classified into upper-tract urothelial cancer (UTUC), affecting the calicopyelic cavities and ureters, and lower-tract urothelial carcinoma (LTUC), including the bladder (90–95%) and proximal urethra. Cystoscopy is the definitive method for diagnosing bladder cancer. Nonetheless, URO-CT is less efficient in detecting LTUC but is beneficial for monitoring muscle-invasive and metastatic bladder

cancer, particularly in evaluating tumor extent, numerous high-risk tumors, or tumors located in the trigone vesica region. In contrast, CT urography exhibits a high sensitivity for the detection of UTUC [1,69,70]. Dual-energy CT (DECT) has emerged as a potential modality for diagnosing and monitoring ulcerative colitis (UC), with benefits such as less exposure to ionizing radiation and iodinated contrast agents [71,72]. Ulcerative colitis may manifest on CT as minor filling deficiencies, mass lesions, vegetations, or wall thickening [71]. The identification of UC depends on the contrast between the tumor and the neighboring non-pathological urothelial wall or surrounding urine. In the parenchymal phase of contrast enhancement, UC generally exhibits heightened enhancement, whereas urine remains unenhanced, and the adjacent normal urothelium shows modest enhancement. During the urographic phase, UC demonstrates diminished enhancement and appears hypodense, whereas iodinated urine exhibits high density. The most significant contrast is noted during the corticomedullary phase, because to the considerable vascularity of UC. During this phase, any region exhibiting urothelial hyperenhancement should be regarded as potentially malignant [73,74].

DECT offers a significant benefit by minimizing radiation exposure via virtual non-contrast (VNC) imaging, obviating the necessity for baseline scans following post-contrast capture, and excluding iodine from soft tissues [7,75]. Additionally, the integration of VNC pictures with the split-bolus strategy has been suggested to further minimize radiation exposure [70]. This procedure simultaneously acquires nephrographic and excretory phases. The contrast media is administered in two distinct portions: the initial portion (often one-third or one-half) is injected, followed by a subsequent portion (normally equal to or exceeding the first) approximately 5–10 minutes later. Nephrographic and excretory-phase pictures are subsequently obtained at 2–5 minutes, during which the renal parenchyma exhibits enhancement [12]. The precise ratio of the initial to the subsequent contrast sections, together with the optimal delay duration, may differ across research [12]. This technique facilitates precise assessment of renal masses and urothelial carcinoma through the concurrent visualization of the cortico-medullary, nephrographic, and excretory phases in one scan [76,77].

A further advantage of DECT is the decreased volume of contrast material used, which is especially beneficial for patients requiring numerous follow-ups or those with renal failure or multiple comorbidities. This is achievable through the utilization of low-energy images that yield higher contrast, attributed to elevated attenuation coefficients at reduced energy levels, thereby enhancing tumor visibility [7]. Low-dose virtual monochromatic imaging (VMI) also facilitates superior quantitative evaluation of primary UC in comparison to traditional venous-phase imaging, while maintaining comparable qualitative outcomes for both primary UC and metastases [79]. DECT also alleviates beam-hardening artifacts induced by metal prostheses, which can skew pelvic assessments. VMI at energy levels ranging from 105 keV to 150 keV mitigates these distortions, while it may affect contrast and soft tissue assessment, necessitating noise reduction. Employing reconstruction techniques that utilize information from various energy levels might further address these problems [80,81,82,83,84,85].

Study of Bladder and Ureters - Limitations of Dual-Energy CT (DECT)

Urothelial tumors (UC) exhibit distinctive features during contrast-enhanced imaging, especially during the nephrographic phase, where the tumors typically show moderate enhancement. In contrast, the surrounding healthy urothelial tissue displays poor enhancement, and the urine remains hypodense. One of the most common diagnostic signs of urothelial tumors is the presence of a filling defect during the pyelographic phase, as highlighted by recent studies. The sensitivity of CT in detecting these tumors can be improved by considering early enhancement as a key diagnostic criterion [85]. Research by Nakagawa et al. [86] demonstrated that virtual monochromatic images (VMI) at 40 keV yielded a significantly higher CT number difference between bladder cancer and the bladder wall compared to synthetic 120 kVp reconstructions. These VMI images were preferred by readers, with statistically significant differences in tumor detection. Similarly, another study found that the contrast-to-noise ratio of urothelial carcinoma relative to the adjacent bladder wall was significantly higher in excretory-phase VMIs at 40 keV compared to conventional venous-phase CT scans [79]. Hansen et al. [87] proposed a dedicated protocol involving a

dual-energy 35-second arterial phase and an 8-minute nephrographic-excretory phase, which showed a sensitivity of 97.3% for detecting urothelial tumors.

Limitations of Dual-Energy CT

Despite its advantages, DECT has several limitations:

- 1. **Simultaneous Data Acquisition Requirement**: For accurate analysis, high- and low-energy data must be acquired simultaneously or within a small time interval. If there is a prolonged gap (e.g., due to patient movement, gastrointestinal peristalsis, or contrast material flow), spatial mismatches between the datasets can degrade image quality. Additionally, the energy difference between the two datasets should be large; a smaller difference leads to lower contrast-to-noise ratios, affecting image clarity.
- 2. **Radiation Exposure**: One of the primary concerns with DECT and CT imaging in general is radiation exposure. According to the International Commission on Radiological Protection (ICRP) standards, radiation exposure should not exceed 50 mSv per year or 100 mSv over a 5-year period [88]. Although a single CT scan typically does not exceed these thresholds, conditions like nephrolithiasis often result in lifelong imaging needs, leading to cumulative radiation exposure over time. One solution to this issue is the use of a **tin filter**, which reduces radiation exposure by absorbing low-energy photons that offer limited diagnostic utility. Second-generation DECT scanners equipped with a tin filter have shown to be effective in reducing radiation exposure [89].
- o **Radiation Dose Studies**: Studies such as those by Apfaltrer et al. and Nestler et al. have reported that using a tin filter and low-dose protocols resulted in high image quality with reduced radiation doses. The mean overall effective doses were 3.34 ± 1.84 mSv and 3.38 ± 1.93 mSv, respectively [90,38]. Dewes et al. also found that using a tin filter reduced radiation exposure by 23%, decreased background noise, and improved image quality when compared to DECT without a tin filter [91].

3. Image Quality Issues:

- Texture and Resolution: VNC images may suffer from rough textures or poor spatial resolution, which can
 make them difficult for radiologists to interpret. In some cases, the images may appear too smooth,
 diminishing their diagnostic value [58,92,93].
- Incomplete Iodine Removal: In cases of high iodine concentration, VNC images may fail to completely remove iodine, leading to incomplete imaging and affecting the detection of small calcifications or renal masses.
- **Higher Noise**: The process of VNC reconstruction can lead to higher image noise, which reduces the visibility and interpretation of renal lesions, especially for small calcifications in kidney masses [4].
- 4. **Obesity-Related Issues**: DECT may be contraindicated in obese patients, as larger body sizes result in greater image noise due to the limited number of photons reaching the detectors. This can reduce image quality and impair material decomposition, thus hindering accurate tissue characterization. Additionally, beam hardening artifacts are more prominent in obese individuals due to the longer path of X-ray attenuation [94,95]. Patient selection for DECT should be carefully assessed based on the patient's body size as observed in the scout radiograph [96].
- 5. **Cost**: The acquisition cost of DECT scanners is a significant limitation. While 16-slice CT scanners typically cost around USD 402,000, and 64- and 80-slice scanners range from USD 549,000, a DECT scanner can cost around USD 1.29 million or even more, making it a costly investment for healthcare systems [97].

In conclusion, while DECT offers several benefits in diagnosing and evaluating urothelial tumors, it also presents challenges, particularly in terms of image quality, patient suitability, and cost. Balancing these factors is crucial for optimizing its clinical use.

Conclusion:

In conclusion, dual-energy computed tomography (DECT) has significantly advanced the field of urological diagnostic imaging by offering enhanced tissue characterization and improved diagnostic accuracy compared to traditional single-energy CT. Its ability to utilize two different energy levels enables better differentiation of materials with distinct elemental compositions, such as the differentiation between uric acid stones and non-uric acid stones. This ability is crucial in accurately diagnosing nephrolithiasis and guiding appropriate treatment decisions. One of the key advantages of DECT is the production of virtual monochromatic images (VMIs), which replicate monochromatic X-ray images at specific energy levels. These images enhance the visibility of contrast-enhanced lesions, reduce noise, and allow for lower contrast medium usage, benefiting patients with renal insufficiency. Additionally, the generation of virtual noncontrast images (VNC) reduces radiation exposure, making DECT an attractive alternative to traditional unenhanced CT scans when such images are necessary. Iodine maps generated by DECT offer another critical clinical tool, providing detailed information on the distribution of iodine in tissues. This feature is particularly useful in identifying tumors, evaluating blood vessels, and assessing therapeutic responses. The ability to differentiate between iodine-enhanced and non-enhanced tissues is invaluable for detecting conditions such as hypervascular lesions, blood vessel abnormalities, and urinary tract injuries. In the clinical setting, DECT has shown promising results in distinguishing between different types of urinary stones, with studies demonstrating high sensitivity and specificity for identifying uric acid stones. The three-material decomposition method employed by DECT, which distinguishes between water, calcium, and uric acid, significantly improves diagnostic accuracy and treatment planning. Furthermore, DECT has been shown to reduce radiation exposure by up to 40% when compared to traditional CT, offering an important advantage for patient safety. Overall, DECT's clinical applications in urology, particularly in the characterization of urinary stones and the evaluation of other genitourinary disorders, underscore its potential as a valuable tool in enhancing diagnostic precision and optimizing patient care. Its ability to provide superior imaging, lower radiation doses, and assist in the differentiation of various materials positions DECT as a critical technology in modern diagnostic radiology.

References:

- Ascenti, G.; Cicero, G.; Bertelli, E.; Papa, M.; Gentili, F.; Ciccone, V.; Manetta, R.; Gandolfo, N.; Cardone, G.; Miele, V. CT-Urography: A Nationwide Survey by the Italian Board of Urogenital Radiology. *Radiol. Med.* 2022, 127, 577–588.
- 2. Joffe, S.A.; Servaes, S.; Okon, S.; Horowitz, M. Multi-Detector Row CT Urography in the Evaluation of Hematuria. *Radiogr. Rev. Publ. Radiol. Soc. N. Am. Inc.* **2003**, *23*, 1441–1455, Discussion in 1455–1456.
- 3. Cicero, G.; Mazziotti, S.; Silipigni, S.; Blandino, A.; Cantisani, V.; Pergolizzi, S.; D'Angelo, T.; Stagno, A.; Maimone, S.; Squadrito, G.; et al. Dual-Energy CT Quantification of Fractional Extracellular Space in Cirrhotic Patients: Comparison between Early and Delayed Equilibrium Phases and Correlation with Oesophageal Varices. *Radiol. Med.* **2021**, *126*, 761–767.
- 4. Kaza, R.K.; Platt, J.F.; Megibow, A.J. Dual-Energy CT of the Urinary Tract. Abdom. Imaging 2013, 38, 167-179.
- 5. Tatsugami, F.; Higaki, T.; Nakamura, Y.; Honda, Y.; Awai, K. Dual-Energy CT: Minimal Essentials for Radiologists. *Jpn. J. Radiol.* **2022**, *40*, 547–559
- 6. Matsumoto, K.; Jinzaki, M.; Tanami, Y.; Ueno, A.; Yamada, M.; Kuribayashi, S. Virtual Monochromatic Spectral Imaging with Fast Kilovoltage Switching: Improved Image Quality as Compared with That Obtained with Conventional 120-KVp CT. *Radiology* **2011**, *259*, 257–262.
- 7. Yang, L.; Sun, J.; Li, J.; Peng, Y. Dual-Energy Spectral CT Imaging of Pulmonary Embolism with Mycoplasma Pneumoniae Pneumonia in Children. *Radiol. Med.* **2022**, *127*, 154–161.
- 8. McCollough, C.H.; Leng, S.; Yu, L.; Fletcher, J.G. Dual- and Multi-Energy CT: Principles, Technical Approaches, and Clinical Applications. *Radiology* **2015**, *276*, 637–653.
- 9. Mileto, A.; Sofue, K.; Marin, D. Imaging the Renal Lesion with Dual-Energy Multidetector CT and Multi-Energy Applications in Clinical Practice: What Can It Truly Do for You? *Eur. Radiol.* **2016**, *26*, 3677–3690.

- 10. Ergun, D.L.; Mistretta, C.A.; Brown, D.E.; Bystrianyk, R.T.; Sze, W.K.; Kelcz, F.; Naidich, D.P. Single-Exposure Dual-Energy Computed Radiography: Improved Detection and Processing. *Radiology* **1990**, *174*, 243–249.
- 11. Fernández-Pérez, G.C.; Fraga Piñeiro, C.; Oñate Miranda, M.; Díez Blanco, M.; Mato Chaín, J.; Collazos Martínez, M.A. Dual-Energy CT: Technical Considerations and Clinical Applications. *Radiol. Engl. Ed.* **2022**, *64*, 445–455
- 12. Cellina, M.; Cè, M.; Rossini, N.; Cacioppa, L.M.; Ascenti, V.; Carrafiello, G.; Floridi, C. Computed Tomography Urography: State of the Art and Beyond. *Tomography* **2023**, *9*, 909–930.
- Pomerantz, S.R.; Kamalian, S.; Zhang, D.; Gupta, R.; Rapalino, O.; Sahani, D.V.; Lev, M.H. Virtual Monochromatic Reconstruction of Dual-Energy Unenhanced Head CT at 65–75 KeV Maximizes Image Quality Compared with Conventional Polychromatic CT. *Radiology* 2013, 266, 318–325.
- 14. Yuan, R.; Shuman, W.P.; Earls, J.P.; Hague, C.J.; Mumtaz, H.A.; Scott-Moncrieff, A.; Ellis, J.D.; Mayo, J.R.; Leipsic, J.A. Reduced Iodine Load at CT Pulmonary Angiography with Dual-Energy Monochromatic Imaging: Comparison with Standard CT Pulmonary Angiography—A Prospective Randomized Trial. *Radiology* **2012**, *262*, 290–297.
- 15. Agrawal, M.D.; Pinho, D.F.; Kulkarni, N.M.; Hahn, P.F.; Guimaraes, A.R.; Sahani, D.V. Oncologic Applications of Dual-Energy CT in the Abdomen. *RadioGraphics* **2014**, *34*, 589–612.
- 16. De Cecco, C.N.; Darnell, A.; Rengo, M.; Muscogiuri, G.; Bellini, D.; Ayuso, C.; Laghi, A. Dual-Energy CT: Oncologic Applications. *AJR Am. J. Roentgenol.* **2012**, *199* (Suppl. S5), S98–S105.
- 17. Silva, A.C.; Morse, B.G.; Hara, A.K.; Paden, R.G.; Hongo, N.; Pavlicek, W. Dual-Energy (Spectral) CT: Applications in Abdominal Imaging. *Radiogr. Rev. Publ. Radiol. Soc. N. Am. Inc.* **2011**, *31*, 1031–1046, Discussion in 1047–1050.
- 18. Ferda, J.; Novák, M.; Mírka, H.; Baxa, J.; Ferdová, E.; Bednárová, A.; Flohr, T.; Schmidt, B.; Klotz, E.; Kreuzberg, B. The Assessment of Intracranial Bleeding with Virtual Unenhanced Imaging by Means of Dual-Energy CT Angiography. *Eur. Radiol.* **2009**, *19*, 2518–2522.
- 19. Hartman, R.; Kawashima, A.; Takahashi, N.; Silva, A.; Vrtiska, T.; Leng, S.; Fletcher, J.; McCollough, C. Applications of Dual-Energy CT in Urologic Imaging: An Update. *Radiol. Clin.* **2012**, *50*, 191–205.
- 20. Nakamura, Y.; Higaki, T.; Honda, Y.; Tatsugami, F.; Tani, C.; Fukumoto, W.; Narita, K.; Kondo, S.; Akagi, M.; Awai, K. Advanced CT Techniques for Assessing Hepatocellular Carcinoma. *Radiol. Med.* **2021**, *126*, 925–935.
- 21. Hamid, S.; Nicolaou, S.; Khosa, F.; Andrews, G.; Murray, N.; Abdellatif, W.; Qamar, S.R. Dual-Energy CT: A Paradigm Shift in Acute Traumatic Abdomen. *Can. Assoc. Radiol. J.* **2020**, *71*, 371–387.
- 22. Nogel, S.J.; Ren, L.; Yu, L.; Takahashi, N.; Froemming, A.T. Feasibility of Dual-Energy Computed Tomography Imaging of Gadolinium-Based Contrast Agents and Its Application in Computed Tomography Cystography: An Exploratory Study to Assess an Alternative Option When Iodinated Contrast Agents Are Contraindicated. *J. Comput. Assist. Tomogr.* **2021**, *45*, 691–695.
- 23. Smith, R.C.; Verga, M.; McCarthy, S.; Rosenfield, A.T. Diagnosis of Acute Flank Pain: Value of Unenhanced Helical CT. *Am. J. Roentgenol.* **1996**, *166*, 97–101.
- 24. Ciccarese, F.; Brandi, N.; Corcioni, B.; Golfieri, R.; Gaudiano, C. Complicated Pyelonephritis Associated with Chronic Renal Stone Disease. *Radiol. Med.* **2021**, *126*, 505–516.
- 25. Andrabi, Y.; Patino, M.; Das, C.J.; Eisner, B.; Sahani, D.V.; Kambadakone, A. Advances in CT Imaging for Urolithiasis. *Indian J. Urol.* **2015**, *31*, 185.
- Nakada, S.Y.; Hoff, D.G.; Attai, S.; Heisey, D.; Blankenbaker, D.; Pozniak, M. Determination of Stone Composition by Noncontrast Spiral Computed Tomography in the Clinical Setting. *Urology* 2000, 55, 816–819.

- 27. Shahnani, P.S.; Karami, M.; Astane, B.; Janghorbani, M. The Comparative Survey of Hounsfield Units of Stone Composition in Urolithiasis Patients. *J. Res. Med. Sci. Off. J. Isfahan Univ. Med. Sci.* **2014**, *19*, 650–653.
- 28. Ngo, T.C.; Assimos, D.G. Uric Acid Nephrolithiasis: Recent Progress and Future Directions. *Rev. Urol.* **2007**, *9*, 17–27.
- 29. Manglaviti, G.; Tresoldi, S.; Guerrer, C.S.; Di Leo, G.; Montanari, E.; Sardanelli, F.; Cornalba, G. In Vivo Evaluation of the Chemical Composition of Urinary Stones Using Dual-Energy CT. *AJR Am. J. Roentgenol.* **2011**, *197*, W76–W83.
- Joshi, M.; Langan, D.A.; Sahani, D.S.; Kambadakone, A.; Aluri, S.; Procknow, K.; Wu, X.; Bhotika, R.; Okerlund, D.; Kulkarni, N.; et al. Effective Atomic Number Accuracy for Kidney Stone Characterization Using Spectral CT; SPIE: Bellingham, WA, USA, 2010; Available online: https://spie.org/Publications/Proceedings/Paper/10.1117/12.844372?SS0=1 (accessed on 2023).
- 31. Flohr, T.G.; McCollough, C.H.; Bruder, H.; Petersilka, M.; Gruber, K.; Süβ, C.; Grasruck, M.; Stierstorfer, K.; Krauss, B.; Raupach, R.; et al. First Performance Evaluation of a Dual-Source CT (DSCT) System. *Eur. Radiol.* **2006**, *16*, 256–268.
- 32. Mansouri, M.; Aran, S.; Singh, A.; Kambadakone, A.R.; Sahani, D.V.; Lev, M.H.; Abujudeh, H.H. Dual-Energy Computed Tomography Characterization of Urinary Calculi: Basic Principles, Applications and Concerns. *Curr. Probl. Diagn. Radiol.* **2015**, *44*, 496–500.
- 33. Thomas, C.; Patschan, O.; Ketelsen, D.; Tsiflikas, I.; Reimann, A.; Brodoefel, H.; Buchgeister, M.; Nagele, U.; Stenzl, A.; Claussen, C.; et al. Dual-Energy CT for the Characterization of Urinary Calculi: In Vitro and in Vivo Evaluation of a Low-Dose Scanning Protocol. *Eur. Radiol.* **2009**, *19*, 1553–1559.
- 34. Jepperson, M.A.; Cernigliaro, J.G.; Ibrahim, E.-S.H.; Morin, R.L.; Haley, W.E.; Thiel, D.D. In Vivo Comparison of Radiation Exposure of Dual-Energy CT Versus Low-Dose CT Versus Standard CT for Imaging Urinary Calculi. *J. Endourol.* **2015**, *29*, 141–146.
- 35. Spek, A.; Strittmatter, F.; Graser, A.; Kufer, P.; Stief, C.; Staehler, M. Dual Energy Can Accurately Differentiate Uric Acid-Containing Urinary Calculi from Calcium Stones. *World J. Urol.* **2016**, *34*, 1297–1302.
- 36. Lombardo, F.; Bonatti, M.; Zamboni, G.A.; Avesani, G.; Oberhofer, N.; Bonelli, M.; Pycha, A.; Mucelli, R.P.; Bonatti, G. Uric Acid versus Non-Uric Acid Renal Stones: In Vivo Differentiation with Spectral CT. *Clin. Radiol.* **2017**, *72*, 490–496.
- 37. Bonatti, M.; Lombardo, F.; Zamboni, G.A.; Pernter, P.; Pycha, A.; Mucelli, R.P.; Bonatti, G. Renal Stones Composition in vivo Determination: Comparison between 100/Sn140 KV Dual-Energy CT and 120 KV Single-Energy CT. *Urolithiasis* 2017, 45, 255–261.
- 38. Nestler, T.; Nestler, K.; Neisius, A.; Isbarn, H.; Netsch, C.; Waldeck, S.; Schmelz, H.U.; Ruf, C. Diagnostic Accuracy of Third-Generation Dual-Source Dual-Energy CT: A Prospective Trial and Protocol for Clinical Implementation. *World, J. Urol.* **2019**, *37*, 735–741.
- 39. Euler, A.; Wullschleger, S.; Sartoretti, T.; Müller, D.; Keller, E.X.; Lavrek, D.; Donati, O. Dual-Energy CT Kidney Stone Characterization—Can Diagnostic Accuracy Be Achieved at Low Radiation Dose? *Eur. Radiol.* **2023**. *Epub ahead of print*
- 40. Kordbacheh, H.; Baliyan, V.; Uppot, R.N.; Eisner, B.H.; Sahani, D.V.; Kambadakone, A.R. Dual-Source Dual-Energy CT in Detection and Characterization of Urinary Stones in Patients with Large Body Habitus: Observations in a Large Cohort. *Am. J. Roentgenol.* **2019**, *212*, 796–801.
- 41. Kordbacheh, H.; Baliyan, V.; Singh, P.; Eisner, B.H.; Sahani, D.V.; Kambadakone, A.R. Rapid KVp Switching Dual-Energy CT in the Assessment of Urolithiasis in Patients with Large Body Habitus: Preliminary Observations on Image Quality and Stone Characterization. *Abdom. Radiol.* **2019**, *44*, 1019–1026.

- 42. Takahashi, N.; Hartman, R.P.; Vrtiska, T.J.; Kawashima, A.; Primak, A.N.; Dzyubak, O.P.; Mandrekar, J.N.; Fletcher, J.G.; McCollough, C.H. Dual-Energy CT Iodine-Subtraction Virtual Unenhanced Technique to Detect Urinary Stones in an Iodine-Filled Collecting System: A Phantom Study. *AJR Am. J. Roentgenol.* **2008**, *190*, 1169–1173.
- 43. Moon, J.W.; Park, B.K.; Kim, C.K.; Park, S.Y. Evaluation of Virtual Unenhanced CT Obtained from Dual-Energy CT Urography for Detecting Urinary Stones. *Br. J. Radiol.* **2012**, *85*, e176–e181.
- 44. Wang, J.; Qu, M.; Leng, S.; McCollough, C.H. Differentiation of Uric Acid versus Non-Uric Acid Kidney Stones in the Presence of Iodine Using Dual-Energy CT. In Proceedings of the SPIE Medical Imaging, San Diego, CA, USA, 13–18 February 2010; Volume 7622.
- 45. Yeo, Y.J.; Kim, S.H.; Kim, M.J.; Kim, Y.H.; Cho, S.H.; Lee, E.J. Diagnostic Efficiency of Split-Bolus Dual-Energy Computed Tomography for Patients with Suspected Urinary Stones. *J. Comput. Assist. Tomogr.* **2015**, *39*, 25–31.
- 46. Magistro, G.; Bregenhorn, P.; Krauß, B.; Nörenberg, D.; D'Anastasi, M.; Graser, A.; Weinhold, P.; Strittmatter, F.; Stief, C.G.; Staehler, M. Optimized Management of Urolithiasis by Coloured Stent-Stone Contrast Using Dual-Energy Computed Tomography (DECT). *BMC Urol.* **2019**, *19*, 29.
- 47. Jepperson, M.A.; Cernigliaro, J.G.; Sella, D.; Ibrahim, E.; Thiel, D.D.; Leng, S.; Haley, W.E. Dual-Energy CT for the Evaluation of Urinary Calculi: Image Interpretation, Pitfalls and Stone Mimics. *Clin. Radiol.* **2013**, *68*, e707–e714.
- 48. Wisenbaugh, E.S.; Paden, R.G.; Silva, A.C.; Humphreys, M.R. Dual-Energy vs Conventional Computed Tomography in Determining Stone Composition. *Urology* **2014**, *83*, 1243–1247.
- 49. Zhang, G.-M.-Y.; Sun, H.; Xue, H.-D.; Xiao, H.; Zhang, X.-B.; Jin, Z.-Y. Prospective Prediction of the Major Component of Urinary Stone Composition with Dual-Source Dual-Energy CT in Vivo. *Clin. Radiol.* **2016**, *71*, 1178–1183.
- 50. Shalini, S.; Kasi Arunachalam, V.; Kumar Varatharajaperumal, R.; Mehta, P.; Thambidurai, S.; Cherian, M. The Role of Third-Generation Dual-Source Dual-Energy Computed Tomography in Characterizing the Composition of Renal Stones with Infrared Spectroscopy as the Reference Standard. *Pol. J. Radiol.* **2022**, *87*, 172–176.
- 51. Taha, M.; Shawky, M.; Abd Ella, M.D.; Tarek, F. Role of Dual Energy Computed Tomography in Evaluation of Renal Stones. *Med. J. Cairo Univ.* **2021**, *89*, 1349–1357.
- 52. Galluzzo, A.; Danti, G.; Bicci, E.; Mastrorosato, M.; Bertelli, E.; Miele, V. The Role of Dual-Energy CT in the Study of Urinary Tract Tumors: Review of Recent Literature. *Semin. Ultrasound CT MRI* **2023**, *44*, 136–144.
- 53. Graser, A.; Becker, C.R.; Staehler, M.; Clevert, D.A.; Macari, M.; Arndt, N.; Nikolaou, K.; Sommer, W.; Stief, C.; Reiser, M.F.; et al. Single-Phase Dual-Energy CT Allows for Characterization of Renal Masses as Benign or Malignant. *Investig. Radiol.* **2010**, *45*, 399–405.
- 54. Pourvaziri, A.; Mojtahed, A.; Hahn, P.F.; Gee, M.S.; Kambadakone, A.; Sahani, D.V. Renal Lesion Characterization: Clinical Utility of Single-Phase Dual-Energy CT Compared to MRI and Dual-Phase Single-Energy CT. *Eur. Radiol.* **2023**, *33*, 1318–1328
- 55. McGrath, T.A.; Ahmad, F.; Sathiadoss, P.; Haroon, M.; McInnes, M.D.; Bossuyt, P.M.; Schieda, N. Direct Comparison of Diagnostic Accuracy of Fast Kilovoltage Switching Dual-Energy Computed Tomography and Magnetic Resonance Imaging for Detection of Enhancement in Renal Masses. *J. Comput. Assist. Tomogr.* **2022**, *46*, 862–870
- 56. Marcon, J.; Graser, A.; Horst, D.; Casuscelli, J.; Spek, A.; Stief, C.G.; Reiser, M.F.; Rübenthaler, J.; Buchner, A.; Staehler, M. Papillary vs Clear Cell Renal Cell Carcinoma. Differentiation and Grading by Iodine Concentration Using DECT-Correlation with Microvascular Density. *Eur. Radiol.* **2020**, *30*, 1–10.

- 57. Jonisch, A.I.; Rubinowitz, A.N.; Mutalik, P.G.; Israel, G.M. Can High-Attenuation Renal Cysts Be Differentiated from Renal Cell Carcinoma at Unenhanced CT? *Radiology* **2007**, *243*, 445–450.
- 58. Graser, A.; Johnson, T.R.C.; Hecht, E.M.; Becker, C.R.; Leidecker, C.; Staehler, M.; Stief, C.G.; Hildebrandt, H.; Godoy, M.C.B.; Finn, M.E.; et al. Dual-Energy CT in Patients Suspected of Having Renal Masses: Can Virtual Nonenhanced Images Replace True Nonenhanced Images? *Radiology* **2009**, *252*, 433–440.
- 59. Thiravit, S.; Brunnquell, C.; Cai, L.M.; Flemon, M.; Mileto, A. Use of Dual-Energy CT for Renal Mass Assessment. *Eur. Radiol.* **2021**, *31*, 3721–3733.
- 60. Arndt, N.; Staehler, M.; Siegert, S.; Reiser, M.F.; Graser, A. Dual Energy CT in Patients with Polycystic Kidney Disease. *Eur. Radiol.* **2012**, *22*, 2125–2129.
- 61. Cha, D.; Kim, C.K.; Park, J.J.; Park, B.K. Evaluation of Hyperdense Renal Lesions Incidentally Detected on Single-Phase Post-Contrast CT Using Dual-Energy CT. *Br. J. Radiol.* **2016**, *89*, 20150860.
- 62. Ascenti, G.; Mazziotti, S.; Mileto, A.; Racchiusa, S.; Donato, R.; Settineri, N.; Gaeta, M. Dual-Source Dual-Energy CT Evaluation of Complex Cystic Renal Masses. *AJR Am. J. Roentgenol.* **2012**, *199*, 1026–1034.
- 63. Moleesaide, A.; Maneegarn, A.; Kaewlai, R.; Thiravit, S. Virtual Monochromatic Spectral Attenuation Curve Analysis for Evaluation of Incidentally Detected Small Renal Lesions Using Rapid Kilovoltage-Switching Dual-Energy Computed Tomography. *Abdom. Radiol.* **2022**, *47*, 3817–3827.
- 64. Wei, J.; Zhao, J.; Zhang, X.; Wang, D.; Zhang, W.; Wang, Z.; Zhou, J. Analysis of Dual Energy Spectral CT and Pathological Grading of Clear Cell Renal Cell Carcinoma (CcRCC). *PLoS ONE* **2018**, *13*, e0195699.
- 65. Greco, F.; Mallio, C.A. Relationship between Visceral Adipose Tissue and Genetic Mutations (VHL and KDM5C) in Clear Cell Renal Cell Carcinoma. *Radiol. Med.* **2021**, *126*, 645–651.
- 66. Walker, D.; Udare, A.; Chatelain, R.; McInnes, M.; Flood, T.; Schieda, N. Utility of Material-Specific Fat Images Derived from Rapid-KVp-Switch Dual-Energy Renal Mass CT for Diagnosis of Renal Angiomyolipoma. *Acta Radiol.* **2021**, *62*, 1263–1272.
- 67. Çamlıdağ, İ.; Nural, M.S.; Danacı, M.; Özden, E. Usefulness of Rapid KV-Switching Dual Energy CT in Renal Tumor Characterization. *Abdom. Radiol.* **2019**, *44*, 1841–1849.
- 68. Alanee, S.; Dynda, D.I.; Hemmer, P.; Schwartz, B. Low Enhancing Papillary Renal Cell Carcinoma Diagnosed by Using Dual Energy Computerized Tomography: A Case Report and Review of Literature. *BMC Urol.* **2014**, *14*, 102.
- 69. Uroweb—European Association of Urology. Non-Muscle-Invasive Bladder Cancer—Introduction—Uroweb. Available online: https://uroweb.org/guidelines/non-muscle-invasive-bladder-cancer (accessed 2023).
- 70. Takeuchi, M.; McDonald, J.S.; Takahashi, N.; Frank, I.; Thompson, R.H.; King, B.F.; Kawashima, A. Cancer Prevalence and Risk Stratification in Adults Presenting with Hematuria: A Population-Based Cohort Study. *Mayo Clin. Proc. Innov. Qual. Outcomes* **2021**, *5*, 308–319
- 71. De Cecco, C.N.; Buffa, V.; Fedeli, S.; Vallone, A.; Ruopoli, R.; Luzietti, M.; Miele, V.; Rengo, M.; Maurizi Enrici, M.; Fina, P.; et al. Preliminary Experience with Abdominal Dual-Energy CT (DECT): True versus Virtual Nonenhanced Images of the Liver. *Radiol. Med.* **2010**, *115*, 1258–1266.
- 72. Buffa, V.; Solazzo, A.; D'Auria, V.; Del Prete, A.; Vallone, A.; Luzietti, M.; Madau, M.; Grassi, R.; Miele, V. Dual-Source Dual-Energy CT: Dose Reduction after Endovascular Abdominal Aortic Aneurysm Repair. *Radiol. Med.* **2014**, *119*, 934–941.
- 73. Helenius, M.; Dahlman, P.; Magnusson, M.; Lönnemark, M.; Magnusson, A. Contrast Enhancement in Bladder Tumors Examined with CT Urography Using Traditional Scan Phases. *Acta Radiol.* **2014**, *55*, 1129–1136.
- 74. Raman, S.P.; Fishman, E.K. Bladder Malignancies on CT: The Underrated Role of CT in Diagnosis. *Am. J. Roentgenol.* **2014**, *203*, 347–354.

- 75. Sahni, V.A.; Shinagare, A.B.; Silverman, S.G. Virtual Unenhanced CT Images Acquired from Dual-Energy CT Urography: Accuracy of Attenuation Values and Variation with Contrast Material Phase. *Clin. Radiol.* **2013**, *68*, 264–271.
- 76. Chow, L.C.; Kwan, S.W.; Olcott, E.W.; Sommer, G. Split-Bolus MDCT Urography with Synchronous Nephrographic and Excretory Phase Enhancement. *AJR Am. J. Roentgenol.* **2007**, *189*, 314–322.
- 77. Chen, C.-Y.; Tsai, T.-H.; Jaw, T.-S.; Lai, M.-L.; Chao, M.-F.; Liu, G.-C.; Hsu, J.-S. Diagnostic Performance of Split-Bolus Portal Venous Phase Dual-Energy CT Urography in Patients with Hematuria. *AJR Am. J. Roentgenol.* **2016**, *206*, 1013–1022.
- 78. Johnson, T.R.C. Dual-Energy CT: General Principles. AJR Am. J. Roentgenol. 2012, 199 (Suppl. S5), S3-S8.
- 79. Zopfs, D.; Laukamp, K.R.; dos Santos, D.P.; Sokolowski, M.; Hokamp, N.G.; Maintz, D.; Borggrefe, J.; Persigehl, T.; Lennartz, S. Low-KeV Virtual Monoenergetic Imaging Reconstructions of Excretory Phase Spectral Dual-Energy CT in Patients with Urothelial Carcinoma: A Feasibility Study. *Eur. J. Radiol.* **2019**, *116*, 135–143.
- 80. Uroweb—European Association of Urology. EAU Guidelines on Upper Urinary Tract Urothelial Cell Carcinoma—Introduction—Uroweb. Available online: https://uroweb.org/guidelines/upper-urinary-tract-urothelial-cell-carcinoma (accessed on 2023).
- 81. Lee, K.Y.G.; Cheng, H.M.J.; Chu, C.Y.; Tam, C.W.A.; Kan, W.K. Metal Artifact Reduction by Monoenergetic Extrapolation of Dual-Energy CT in Patients with Metallic Implants. *J. Orthop. Surg.* **2019**, *27*, 2309499019851176.
- 82. Bamberg, F.; Dierks, A.; Nikolaou, K.; Reiser, M.F.; Becker, C.R.; Johnson, T.R.C. Metal Artifact Reduction by Dual Energy Computed Tomography Using Monoenergetic Extrapolation. *Eur. Radiol.* **2011**, *21*, 1424–1429.
- 83. Lewis, M.; Reid, K.; Toms, A.P. Reducing the Effects of Metal Artefact Using High KeV Monoenergetic Reconstruction of Dual Energy CT (DECT) in Hip Replacements. *Skelet. Radiol.* **2013**, *42*, 275–282.
- 84. Higashigaito, K.; Angst, F.; Runge, V.M.; Alkadhi, H.; Donati, O.F. Metal Artifact Reduction in Pelvic Computed Tomography with Hip Prostheses: Comparison of Virtual Monoenergetic Extrapolations from Dual-Energy Computed Tomography and an Iterative Metal Artifact Reduction Algorithm in a Phantom Study. *Investig. Radiol.* **2015**, *50*, 828–834.
- 85. Bicci, E.; Mastrorosato, M.; Danti, G.; Lattavo, L.; Bertelli, E.; Cozzi, D.; Pradella, S.; Agostini, S.; Miele, V. Dual-Energy CT Applications in Urinary Tract Cancers: An Update. *Tumori* **2023**, *109*, 148–156.
- 86. Nakagawa, M.; Naiki, T.; Naiki-Ito, A.; Ozawa, Y.; Shimohira, M.; Ohnishi, M.; Shibamoto, Y. Usefulness of Advanced Monoenergetic Reconstruction Technique in Dual-Energy Computed Tomography for Detecting Bladder Cancer. *Jpn. J. Radiol.* **2022**, *40*, 177–183.
- 87. Hansen, C.; Becker, C.D.; Montet, X.; Botsikas, D. Diagnosis of Urothelial Tumors with a Dedicated Dual-Source Dual-Energy MDCT Protocol: Preliminary Results. *Am. J. Roentgenol.* **2014**, *202*, W357–W364.
- 88. Wrixon, A.D. New ICRP Recommendations. J. Radiol. Prot. 2008, 28, 161–168.
- 89. Agostini, A.; Borgheresi, A.; Carotti, M.; Ottaviani, L.; Badaloni, M.; Floridi, C.; Giovagnoni, A. Third-Generation Iterative Reconstruction on a Dual-Source, High-Pitch, Low-Dose Chest CT Protocol with Tin Filter for Spectral Shaping at 100 KV: A Study on a Small Series of COVID-19 Patients. *Radiol. Med.* **2021**, *126*, 388–398.
- 90. Apfaltrer, G.; Dutschke, A.; Baltzer, P.A.T.; Schestak, C.; Özsoy, M.; Seitz, C.; Veser, J.; Petter, E.; Helbich, T.H.; Ringl, H.; et al. Substantial Radiation Dose Reduction with Consistent Image Quality Using a Novel Low-Dose Stone Composition Protocol. *World J. Urol.* **2020**, *38*, 2971–2979.
- 91. Dewes, P.; Frellesen, C.; Scholtz, J.-E.; Fischer, S.; Vogl, T.J.; Bauer, R.W.; Schulz, B. Low-Dose Abdominal Computed Tomography for Detection of Urinary Stone Disease—Impact of Additional Spectral Shaping of the X-ray Beam on Image Quality and Dose Parameters. *Eur. J. Radiol.* **2016**, *85*, 1058–1062.

- 92. Marin, D.; Boll, D.T.; Mileto, A.; Nelson, R.C. State of the Art: Dual-Energy CT of the Abdomen. *Radiology* **2014**, *271*, 327–342.
- 93. Mileto, A.; Marin, D.; Nelson, R.C.; Ascenti, G.; Boll, D.T. Dual Energy MDCT Assessment of Renal Lesions: An Overview. *Eur. Radiol.* **2014**, *24*, 353–362.
- 94. Parakh, A.; An, C.; Lennartz, S.; Rajiah, P.; Yeh, B.M.; Simeone, F.J.; Sahani, D.V.; Kambadakone, A.R. Recognizing and Minimizing Artifacts at Dual-Energy CT. *Radiogr. Rev. Publ. Radiol. Soc. N. Am. Inc.* **2021**, *41*, 509–523.
- 95. Lambert, J.W.; FitzGerald, P.F.; Edic, P.M.; Sun, Y.; Bonitatibus, P.J.; Colborn, R.E.; Yeh, B.M. The Effect of Patient Diameter on the Dual-Energy Ratio of Selected Contrast-Producing Elements. *J. Comput. Assist. Tomogr.* **2017**, *41*, 505–510.
- 96. Borges, A.P.; Antunes, C.; Curvo-Semedo, L. Pros and Cons of Dual-Energy CT Systems: "One Does Not Fit All". *Tomography* **2023**, *9*, 195–216.
- 97. Dual-Energy CT: Is It What the Doctor Ordered for the Cost-Conscious Community Hospital? Available online: https://radiologybusiness.com/sponsored/1081/hitachi-healthcare-americas/topics/healthcare-management/healthcare-economics/dual (accessed on 2023). تنظييقات الناشئة للتصوير المقطعي المحوسب ذو الطاقة المزدوجة في الأشعة التشخيصية مراجعة محدثة لتقييم أمراض المسالك البولية

الملخص:

الخلفية :لقد ظهرت تقنيات التصوير المقطعي المحوسب ذو الطاقة المزدوجة (DECT) كتقنية تصوير متقدمة في الأشعة التشخيصية، خصوصًا في تقييم المسالك البولية. حيث تتغلب هذه التقنية على العديد من القيود التي كانت موجودة في التصوير المقطعي التقليدي من خلال استخدام مستويين مختلفين للطاقة، مما يوفر تحسينًا في تصنيف الأنسجة ودقة أكبر في التباين. لقد أظهرت DECT وعدًا كبيرًا في تقييم أمراض المسالك البولية، حيث توفر بيانات دقيقة عن التركيب والشكل والوظيفة، مما يعزز من اتخاذ القرارات السربرية.

الهدف :تهدف هذه المراجعة إلى استكشاف المبادئ والفوائد والتطبيقات السريرية لتقنية DECT في تقييم اضطرابات المسالك البولية، مع التركيز بشكل خاص على تصنيف الحصوات البولية.

الطرق : تستعرض هذه المراجعة بيانات من دراسات مختلفة تبحث في استخدام DECT في تصوير المسالك البولية، مع التركيز على تحليل الحصوات البولية. كما يتم مناقشة تقنيات DECT المختلفة مثل التصوير المقطعي ذو المصدرين والتصوير الطيفي، مع تسليط الضوء على قدرتها على التمييز بين تركيبات الحصوات وأهميتها السربرية.

النتائج: تقدم DECT العديد من المزايا في تقييم المسالك البولية، مثل الصور الأحادية اللون الافتراضية (VMIs)، والصور الافتراضية غير المحسنة بالتباين، وخرائط اليود، ومنحنيات وحدات هونسفيلد الطيفية (HU) تعزز هذه القدرات من الكشف عن الحصوات البولية وتصنيفها، بما في ذلك التمييز بين حصوات حمض اليوريك والحصوات غير حمض اليوريك بدقة عالية. أظهرت الدراسات أن DECT يوفر دقة تشخيصية أعلى مقارنة بالتقنيات التقليدية، خصوصًا في تحديد تركيب الحصوات، وبقلل من التعرض للإشعاع.

الخلاصة :تمثل DECT تقدمًا كبيرًا في تصوير المسالك البولية التشخيصي، مما يحسن دقة تصنيف الحصوات البولية، ويقلل من التعرض للإشعاع، ويوفر تحليلًا شاملًا للأنسجة. كما يعزز من إدارة المرضى السربرية من خلال تمكين التمييز الدقيق بين أنواع الحصوات وتحسين استراتيجيات العلاج.

الكلمات المفتاحية :التصوير المقطعي ذو الطاقة المزدوجة، المسالك البولية، الحصوات البولية، الأشعة التشخيصية، الصور الأحادية اللون الافتراضية، خرائط اليود، تقليل الإشعاع، تصنيف الأنسجة، حصوات الكلي.